Improvement of Low Traffic Volume Gravel Roads in Nebraska

Yijun Liao
Graduate Research Assistant
Department of Civil and Environmental Engineering
University of Nebraska-Lincoln

Mohammad Ebrahim Mohammadi, Ph.D.
Postdoctoral Research Associate
Department of Civil and Environmental Engineering
University of Nebraska-Lincoln

Richard L. Wood, Ph.D.
Assistant Professor
Department of Civil and Environmental Engineering
University of Nebraska-Lincoln

Yong-Rak Kim, Ph.D.
Professor (formerly held position)
Department of Civil and Environmental Engineering
University of Nebraska-Lincoln

A Report on Research Sponsored by

Nebraska Department of Transportation

University of Nebraska-Lincoln

March 2020

Technical Report Documentation Page

<table>
<tr><td colspan="2">1. Report No

SPR-P1(16) M040</td><td>2. Government Accession No.</td><td colspan="2">3. Recipient's Catalog No.</td></tr>
<tr><td colspan="3" rowspan="2">4. Title and Subtitle
Improvement of Low Traffic Volume Gravel Roads in Nebraska</td><td colspan="2">5. Report Date
January 2020</td></tr>
<tr><td colspan="2">6. Performing Organization Code</td></tr>
<tr><td colspan="3">7. Author(s)
Yijun Liao, Mohammad Ebrahim Mohammadi, Richard L. Wood, and Yong-Rak Kim</td><td colspan="2">8. Performing Organization Report No.</td></tr>
<tr><td colspan="3" rowspan="2">9. Performing Organization Name and Address
University of Nebraska – Lincoln
1400 R Street
Lincoln, NE 68588</td><td colspan="2">10. Work Unit No. (TRAIS)</td></tr>
<tr><td colspan="2">11. Contract or Grant No.
SPR-P1(16) M040</td></tr>
<tr><td colspan="3" rowspan="2">12. Sponsoring Organization Name and Address
Nebraska Department of Transportation
1400 Highway 2
PO BOX 94759
Lincoln, NE 68509</td><td colspan="2">13. Type of Report and Period Covered</td></tr>
<tr><td colspan="2">14. Sponsoring Agency Code</td></tr>
<tr><td colspan="5">15. Supplementary Notes</td></tr>
<tr><td colspan="5">16. Abstract
In the state of Nebraska, over one-third of roadways are unpaved, and consequently require a significant amount of financial and operational resources to maintain their operation. Undesired behavior of surface gravel aggregates and the road surfaces can include rutting, corrugation, and ponding that may lead to reduced driving safety, speed or network efficiency, and fuel economy. This study evaluates the parameters that characterize the performance and condition of gravel roads overtime period related to various aggregate mix designs. The parameters, including width, slope, and crown profiles, are examples of performance criteria. As remote sensing technologies have advanced in the recent decade, various techniques have been introduced to collect high quality, accurate, and dense data efficiently that can be used for roadway performance assessments. Within this study, two remote sensing platforms, including an unpiloted aerial system (UAS) and ground-based lidar scanner, were used to collect point cloud data of selected roadway sites with various mix design constituents and further processed for digital assessments. Within the assessment process, statistical parameters such as standard deviation, mean value, and coefficient of variance are calculated for the extracted crown profiles. In addition, the study demonstrated that the point clouds obtained from both lidar scanners and UAS derived SfM can be used to characterize the roadway geometry accurately and extract critical information accurately.</td></tr>
<tr><td colspan="2">17. Key Words
Gravel road assessment, gravel road aggregates, remote sensing, UAS, lidar, point clouds</td><td colspan="3">18. Distribution Statement</td></tr>
<tr><td>19. Security Classification (of this report)
Unclassified</td><td>20. Security Classification (of this page)
Unclassified</td><td>21. No. Of Pages
70</td><td colspan="2">22. Price</td></tr>
</table>

Table of Contents

List of Figures

List of Tables

ACKNOWLEDGMENTS

Funding for this project was provided by the Nebraska Department of Transportation (NDOT) under project number M040 – Improvement of Low Traffic Volume Gravel Roads in Nebraska. The authors would like to express their gratitude for the support and guidance provided by the NDOT Technical Advisory Committee as well as graduate research assistant Mr. Dan Waston, and undergraduate student assistants, Ms. Alexis Laurent and Ms. Giovana de Brito Silva for assisting in field data collection. Graduate research assistants Mr. Shayan Gholami and Mr. Mohammad Rahmani for leading the aggregate material testing and analysis, and Mr. Peter Hilsabeck of the UNL Structural Laboratory for setup and data collection assistance. The authors would also like to extend their gratitude to Ms. Pam Dingman and Mr. Chad Packard from Lancaster County Engineering for their gracious support of this project, including site selection, material identification, and placement discussion.

DISCLAIMER

The contents of this report reflect the views of the authors, who are responsible for the facts and the accuracy of the information presented herein. The opinions, findings, and conclusions expressed in this publication are those of the authors and not necessarily those of the sponsors. This report does not constitute a standard, specification, or regulation. This material is based upon work supported by the Federal Highway Administration under SPR-P1(16) M040. Any opinions, findings, and conclusions or recommendations expressed in this publication are those of the author(s) and do not necessarily reflect the views of the Federal Highway Administration.

ABSTRACT

In the state of Nebraska, over one-third of roadways are unpaved, and consequently require a significant amount of financial and operational resources to maintain their operation. Undesired behavior of surface gravel aggregates and the road surfaces can include rutting, corrugation, and ponding that may lead to reduced driving safety, speed or network efficiency, and fuel economy. This study evaluates the parameters that characterize the performance and condition of gravel roads overtime period related to various aggregate mix designs. The parameters, including width, slope, and crown profiles, are examples of performance criteria. As remote sensing technologies have advanced in the recent decade, various techniques have been introduced to collect high quality, accurate, and dense data efficiently that can be used for roadway performance assessments. Within this study, two remote sensing platforms, including an unpiloted aerial system (UAS) and ground-based lidar scanner, were used to collect point cloud data of selected roadway sites with various mix design constituents and further processed for digital assessments. Within the assessment process, statistical parameters such as standard deviation, mean value, and coefficient of variance are calculated for the extracted crown profiles. In addition, the study demonstrated that the point clouds obtained from both lidar scanners and UAS derived SfM can be used to characterize the roadway geometry accurately and extract critical information accurately.

CHAPTER 1 – INTRODUCTION

1.1 PROJECT OVERVIEW

In the state of Nebraska, approximately 75% or 72,000 miles of the roads are unpaved. Due to environmental conditions and as well as overwhelming cost and resource-intensive maintenance, the poor performance of gravel roads is commonly observed. Therefore, monitoring these low-volume roadways require a significant amount of resources and manpower to maintain the profile and gravel aggregates. Undesired behavior of such roads includes corrugation and ponding that may lead to reduced driving safety, vehicle speed, and fuel economy. On any roadway system, drainage design is a core part of the road performance, particularly for gravel roads. The improper crown profile geometries can result in drainage problems. Consequently, water cannot be drained efficiently during rainstorms, which often softens the gravel crust. Furthermore, severe rutting can be developed if water penetrates and softens the subgrade. Another possible undesirable behavior is ponding, which is the collection of water at surface depressions.

Compared to traditional methods, point clouds can be collected with increased accuracy and cost and time-efficient approaches. Specifically for areas of interest with limited accessibility, point clouds acquired by remote sensing techniques are an efficient, accurate, and economical approach for objective assessments. Light detection and ranging (lidar) and unpiloted (or unmanned) aerial system (UAS) with onboard camera platforms are two common remote sensing approaches to obtain three-dimensional (3D) point clouds, both of which are utilized in this work.

Within this project, the gravel roads are assessed base on various performance parameters, including elevation, width, drainage crown slopes, and surface roughness, as well as the quality

metrics such as crown slope consistency along the roadway. In addition, the assessments were planned to carry out in different aggregates mix designs over a one-year cycle monitoring. While these mix designs are tested analyzed in the lab and developed based on state manuals, due to the funding limitation, the material placement phase was canceled in this project.

*1.2 **RESEARCH MOTIVATIONS, OBJECTIVES, AND SCOPE***

Gravel road assessment is traditionally performed using manual measurements along the straight edges of a road. These methods are time-consuming, inefficient, and results can be subjective. Manual measurements of gravel roads are subjective due to the location of the placed straight edges, which may produce drastically different measurements due to slight variations in placements. Therefore, alternative methods have been developed to assess gravel roads based on digital surveying technologies such as laser profilometers, laser scanners, and USAs (Giesko et al. 2007; Williams et al. 2013; Brooks et al. 2015). Among these technologies available to assess the gravel roads, ground-based lidar scanning (GBL) and UAS platforms, data can be processed to create 3D point cloud models that can be used for various road surface assessments. Specific to this work, a method is developed to assess the gravel roads based on three-dimensional point cloud data automatically and objectively.

*1.3 **REPORT ORGANIZATION***

This report is divided into five chapters. Chapter 1 provides the project overview, motivations, objectives, and scope of the research. Chapter 2 lists and discusses previous studies related to this project and is divided into subsections for material mix design, previous assessment methodologies, and the application of remote sensing and point cloud data for the assessment of

road surfaces. Chapter 3 presents the mix design evaluation and results and provides a modified mix design that is proposed for a test strip for future testing and confirmation. Chapter 4 details the methodology developed to analyze point clouds for gravel road assessments, the data collection processes, and error analyses used within the proposed method. In addition, the example of datasets and processing results are presented in Chapter 4. Chapter 5 provides the conclusion and recommendation of this report and further discusses the potential future research work for this project. Lastly, the appendix presents all of the datasets collected and processed within this project.

1.4 RESEARCH OBJECTIVES

The following sections outline the research tasks as described in the original proposal.

1.4.1 Literature Review and Preliminary Data Collection

Within this project, initially, a literature review was conducted regarding the effects of aggregate properties on the performance of gravel roads as well as recently proposed methods to collect and analyze remote sensing data of gravel roads and other similar civil infrastructure systems. Afterward, a series of sites were selected throughout the state for remote sensing data collection and to determine the current performance of gravel roads before material testing and placement. This included analyzing samples from the select sites for material characterization.

1.4.2 TAC Meeting and Experimental Planning

The research team met and coordinated with the project technical advisory committee (TAC) for an in-depth discussion of the project. The goal of this task was to determine the

experimental plan to select material, test strip attributes (e.g., length, location), variables affecting the performance of the gravel roads based on the scope of the project, parameters to characterize gravel road and material performance, and methods of assessment and processing remote sensing data.

1.4.3 Material Collection and Characterization

Using resources available for material analysis at the University of Nebraska-Lincoln, the team has collected various aggregate mixes for evaluation. This included the Lancaster County stockpile, aggregates from various commercial gravel pits, and aggregates obtained directly from roadways. The investigated parameters included gradation characteristics (sieve analysis), plasticity index, L.A. abrasion loss, shape/angularity, and surface roughness, etc.

1.4.4 Correlation to Existing Roadway Data

Within this task, the team designed the test strips at the selected sites based on the initial data collection and performance analysis results of the existing roadway and material behavior and characterization. This was performed in coordination with TAC members and county officials. The designed sites were originally planned to be in several locations throughout the state to account for various weather, environmental, and traffic conditions for different gravel aggregate mixtures. However, no test strips were placed due to administration and financial constraints that were outside of the control of the project team.

*1.4.5 **Test Strip Construction***

The test strip was designed, and quantities were estimated to be placed in the nearby vicinity of Lincoln, NE. The test strip was reviewed by TAC and county officials but ultimately was not placed due to constraints and timing outside of the project team's control. Four different gravel mixes were to be evaluated at the test strip using on-site mixing between a typical gravel road mix, deicing gravel, and a cohesion clay material. However, no test strip was constructed due to administration and financial constraints, which were not under management and control of the project team.

*1.4.6 **Test Strip Assessment and Data Collection***

Each test strip was planned to be assessed minimally at each scheduled maintenance or at refined intervals throughout a one-year cycle. This assessment schedule was selected to ensure that the study captures the effect of seasonal changes, including freeze/thaw cycles, heavy spring rains for higher moisture content and potential for washout, and the drier months of July to August. In addition, the study was planned to account for traffic on the test sites. Therefore, traffic counts were intended to be implemented through portable counter systems to quantify the traffic loads (during various intervals of this phase). However, the assessment duration was modified due to the lack of material placement. However, the data collection would have been carried out over a one year cycle to compare the performance of the material was developed. Table 6 in the report later details a temporal comparison which demonstrates the anticipated roadway degradation over a 4-month interval.

*1.4.7 **Correlation of Performance Evaluation Data to Material Characterization***

Within this task, the team proposed to perform analyses to correlate the collected remotely sensed data to the material characteristics of each test strip. This task was to include the development method to analyze the remotely sensed data. Also, the team was to use the analysis results of the correlation to justify a recommended specification based on the observed performance of the gravel road. This was not performed since the test strip was not constructed, this was discussed with NDOT TAC members.

*1.4.8 **Reference Table for Objectives***

This section provides a summary table (Table 1) that outlines how the objectives are further discussed in this report.

Table 1. Project objectives as discussed throughout the report.

Objective	Section(s)
1. Literature review and preliminary data collection	2.1 to 2.5 and 4.1 to 4.4
2. TAC meeting and experimental plan	3.1 to 3.4
3. Material collection and characterization	3.1 and 3.2
4. Correlation to existing roadway data	3.3
5. Test strip construction	3.4
6. Test Strip assessment and data processing	4.1 to 4.5
7. Correlation of performance evaluation data to material characterization	5.1 to 5.4

CHAPTER 2 – LITERATURE REVIEW

Due to the maintenance costs and roadway safety improvement demand, material comparison and recommendation is one of the project's primary goals and focus. Various aggregate sourced from multiple quarries throughout the state has been characterized to identify geometric properties such as sizes, angularity, and gradation characteristics. In addition, site practice and practices were also discussed in the previous studies, which can be modified for in-site material placement procedures.

2.1 GRAVEL ROAD MATERIAL MIX DESIGN AND PRACTICES

The effect of material and different mix designs, as well as site practice (i.e., material placement and maintenance), have previously been studied by various researchers and state agencies to identify optimal mix design and practices. In a similar study, Eggebraaten and Skorseth (2009) evaluated the performance of three types of aggregates. The first aggregate was created according to SDDOT specifications, and the second aggregate specimen was developed based on the SDDOT specifications for the gravel roads standard, which did not meet SDDOT gravel surfacing specifications. The second aggregate contained low particles passing #200 sieve and/or had the plastic index (PI) of 4. The third aggregate was a modified SDDOT spec, which contained 10% particles passing #200 sieve and PI at 7. These three types of aggregates were placed within the three equal sections on the same road. The study reported that, after one month of the material placement, the substandard gravel loosened the most, while the modified material

loosened by about 20%. However, other parameters and characteristics of the test strips such as widths, crown, and corrugation were not quantitatively assessed.

The Nebraska Department of Transportation (2007) specifications indicate that for the surfacing of the gravel roads, gravel passing #200 sieve can be 0 – 6% (by weight) with no plasticity index (PI) required. This standard specification indicates the commonly used material; however, the current state specifications lack the inclusion of fine material that provides for a cohesive behavior of the material. Similarly, the specifications also did not mandate the use of crushed rock within the material, which can increase in angularity to improve the interlocking behavior.

2.2 GRAVEL ROAD ASSESSMENT

As digital technology evolves, the cost of measurement instrumentation is reducing while the capabilities, accuracy, and effective ranges continue to improve. Therefore, many industries, including civil engineering, drove to use sensor-based measurements and monitoring methods. As a result, within the area of road assessments, various methods have been introduced to evaluate the in-situ conditions of roadway surfaces, including inertial-based measurements and vision-based approaches.

One early work using a profilometer for profile measurement was proposed by Yang et al. (2007). The developed surface profile configuration analysis is comprised of a vertical gyro, laser displacement that records movement in the X and Y directions, and a wheel encoder (Yang et al. 2007). However, the road profile measurement device only collects profile data along with the trailer wheel trackers, which limits the profile measurement to the width direction of the roads. However, Yang et al. (2007) reported that the developed method is more reliable, efficient, and

less subjective in comparison to that of manual measurements. More recently, Lee et al. (2017) proposed a methodology to improve the previous profilometer system as used by Yang et al. (2007). Different from the traditional two dimensional (2D) profilometer, a newly-developed 3D profilometer system consists of a computer for data processing, power unit, vehicle measurement unit, and on-vehicular sensors including a wheel encoder and laser scanner. With this updated system, Lee et al. (2017) characterized the road profiles up to a velocity of 6.2 mph (10 km/hr), and it was reported the result of the 3D profilometer only differs by 2% in comparison to those measured in real-world conditions. Lastly, the study concluded that the 3D profilometer platform can produce sufficient accuracy, which extends the potential usage of the model to analyze vehicle durability and fatigue life prediction in addition to road surface assessments. However, these systems are costly and due to their delicate nature, the use on gravel roads is likely not preferred.

*2.3 **REMOTE SENSING ASSESSMENT APPLICATION***

Remote sensing technologies application has proliferated in recent years to acquire 3D point clouds. Remote sensing platforms that use lidar sensors or 3D reconstruction of a scene using UAS collected images are two common remote sensing approaches to obtain 3D point clouds. A point cloud is a set of points in three-dimensional space that represents the surface of objects. Remote sensing platform that uses a lidar sensor is an example of active remote sensing, where data collection occurs via a laser waveform, and distances are computed using the time-of-flight or phase shift of the returned waveform. Numerous benefits can be achieved through lidar scanners such as the ability to conduct objective measurements and assessments with higher accuracy in a semi-autonomous data collection approach while limiting human exposure to the environment. For specific civil infrastructure networks, UAS based photogrammetry and data

collection is an ideal option, particularly given its overhead view of a region of interest. UAS data acquisition includes digital images and georeferencing information that can be processed to produce a point cloud using an advanced computer vision technique, known as structure-from-motion (SfM). SfM uses a series of two-dimensional images with sufficient overlap to estimate the 3D geometry of objects in the scene. Given its efficiency, accuracy, density, and lower-cost, UAS point cloud data acquisition has been widely applied to the areas of transportation, engineering, geology, or surveying.

The UAS derived point clouds have been used previously for digital assessments. Wood and Mohammadi (2015) used a UAS derived point cloud as the supplementary data to minimize lidar point cloud occlusion for the task of structural inspection. Within this study, a lidar scanner was used to create the point cloud models of the walls. However, occlusion exits within the collected GBL data due to the inaccessibility to the roof and other damaged areas due to the unsafe condition of the structure. As a result, the UAS derived point clouds of these hard to reach areas were created and registered to the GBL derived point clouds to create a highly detailed point cloud with minimal occlusion. In addition, the study reported that occlusion in the central area of the façade was nearly 20% for the GBL data while the combined point cloud reduces the area of occlusion to 7.6%. Note that these measurements (percent of occlusion) were computed with respect to reference girds of points. As a result, the proposed methodology to create a combined point cloud dataset provides an efficient solution in terms of safety, time, and accuracy for structural inspection of damaged structures.

In addition to roadway and highway equipment management, lidar technology has been deployed to evaluate the road surface and geometry. Liu et al. (2011) discussed the application of the lidar point cloud data for evaluating the severity of rail-highway hump crossings with respect

to road grade profile and vehicle dimensions. This method starts by updating the point cloud data of the rail-highway hump crossing coordinate system, subsampling, and then computing the elevation map. For a given point cloud dataset and seven example vehicle dimensions, the elevation difference between each vehicle bottom and the pavement surface inputted is evaluated and checked. The results of the method are analyzed to determine if the rail-highway crossing is safe for the example vehicle. The proposed method can accept any vehicle's dimensions; however, no detailed description is provided on how the original data coordinate system is established or subsampled.

In addition to analyzing UAS captured images for damage detection and documentation, these images have been used to reconstruct the 3D scene for structural assessment applications. Galarreta et al. (2015) used high-resolution oblique images collected by a UAS platform to create a 3D point cloud of a scene. Furthermore, the study combined the 3D point cloud data with the results of a developed image analysis technique for building damage assessment. To detect damage in facade and roof components, an object-based image analysis method was developed that used image segmentation and object classification. This method was supplemented by user input. Galarreta et al. (2015) concluded that while the oblique images collected by a UAS platform are suitable for assessments of façade and roof components, their proposed damage detection method was not able to identify all existing damage patterns and further research needs to be performed.

2.4 POINT CLOUD APPLICATION TO THIS PROJECT

In the past decade, vision-based technology has been widely used in the field of civil engineering including structural health monitoring, construction engineering, and transportation applications (Liao et al. 2019). Within the field of transportation engineering, point cloud data

(created by SfM technique or lidar platforms) has been used to update transportation infrastructure inventories, surface defect detection of roadways, drainage analyses, and pavement smoothness evaluations.

In addition to the unpaved gravel road assessment, various studies investigate the application of UAS derived point clouds for road surface assessments. Zhang et al. (2012) presented a method to perform 3D measurement of unpaved road surface distresses. The proposed methodology investigates unpaved road assessment in sub-centimeter accuracy using UAS derived point clouds. This includes parameters of roadway length, potholes, and roadway rutting depth. Zhang et al. (2012) reported that a UAS platform is able to carry out 2D imagery collection faster, more safely and at a lower cost in comparison to satellite and manned aircraft. As a highly flexible data collection platform, UASs can be programmed off-line as well as be controlled in real-time for an operation. Various devices such as interchangeable imaging devices and other sensors are also applicable to be onboard as needed. Within this study, Zhang et al. (2012) were able to detect and measure surface distress without difficulties manually. This methodology was then compared to a case study on rural roads, where the difference between results and actual onsite measurements are with a centimeter.

Dobson et al. (2013) assess unpaved roadway using UAS derived 3D point cloud models. Dobson et al. (2013) used a Tazar 800 helicopter UAS with an onboard camera sensor for the study, and multiple assessment parameters are identified through both 2D images and 3D point cloud models. The parameters include ruts and washboard, which were found by applying the threshold filter function to 2D imagery data and potholes detected and calculated using the Canny edge detection function and Hough Circle Transform in 2D images. Using the 3D reconstructed point cloud, drainage is estimated by the off-road area and the profile is extracted. The opinion of the

authors is that the distress identification process is rapid, accurate, and can be extended to a larger area.

2.5 CONCLUSIONS

As a monitoring method, point clouds have been widely implemented in various infrastructure assessments. This improves efficiency, accessibility, accuracy, and reduce subjectivity that is tied to traditional methods. However, traditional approaches are still commonplace in gravel road assessments. As a result and as one of the goals of this study, a method is developed based on point clouds to assess gravel roads and characterize the surface behavior based on the various aggregate mixtures. Using point clouds will enable an objective and time-efficient method to characterize these low-volume gravel roads.

CHAPTER 3 – MODIFIED GRAVEL ROAD MIX DESIGN

3.1 EXISTING MIX DESIGNS

The existing mix designs used within this project are outlined by the Nebraska Department of Transportation (NDOT) standard specifications. The recommendation design mixture is shown below in Table 2. Within the recommended specifications, no PI is required for cohesion nor angularity for interlocking behavior. In addition, other properties such as shape, angularity, and surface texture are not indicated.

Table 2. Mix designs recommended by NDOT spec.

Sieve	**Crushed Rock for Surfacing (Table 1033.08)**	**Gravel for Surfacing (Table 1033.07)**
	Percentage Passing	
1'' (25.0 mm)	100	100
¾'' (19.0 mm)		
½'' (12.5 mm)		
No. 4 (4.75 mm)	40±20	78±17
No. 8(2.36 mm)		
No. 10 (2.0 mm)	15±15	16
No. 40 (425 µm)		
No. 200 (75 µm)	5±5	3±3
Plastic Index (PI)		
L.A. Abrasion. Loss, max.	45	40
Processing required	Crushed	

3.2 EXISTING AGGREGATES TESTING

Within the state of Nebraska, the existing aggregates that are commonly utilized on the roadway can be obtained from various local quarries or county stockpile. Therefore, samples obtained from these quarries were tested in the UNL material's lab. The tests used are sieve analysis, form, angularity, texture, and PI. After iteration with numerous quarries throughout the state, the recommended gravel mix sample was obtained from Western Sand Gravel in Columbus, Nebraska. The deicing gravel aggregate was selected due to the higher fine material content, which improves the cohesion. The sieve analysis results are presented in Table 3. As shown, the test result meets the standard determined by the NDOT specifications comparing to the sieve passing percentages. To further analyze the aggregate features, an aggregate imaging system (AIMS) was utilized to evaluate the aggregate properties. As a result, the output parameters are: form - first-order property, reflects variations in the proportions of a particle; angularity - second-order property, reflects variations at the corners; surface texture - describes the surface irregularity at a scale that is too small to affect the overall shape. Specific for this sample, the angularity is moderate, the texture is moderate, the sphericity index is high, PI is 1 and LA abrasion is 30.

Table 3. Sieve analysis of the quarry sample.

Sieve No.	Amount Retained (g)	Cumulative Amount Retained (g)	Cumulative Percent Retained	Percent Passing
3/4 in	0	0	0.0	100.0
1/2 in	0	0	0.0	100.0
3/8 in	84.99	84.99	0.4	99.6
#4	3550.04	3635.03	16.0	84.0
#8	6592.5	10227.53	45.0	55.0
#16	3923.47	14151.00	62.2	37.8
#30	3162.44	17313.44	76.1	23.9
#50	3324.70	20638.14	90.8	9.2
#100	1845.50	22483.64	98.9	1.1
#200	229.09	22712.73	99.9	0.1
Pan	25.59	22738.32	100.0	0.0
Total	22738.32			

3.3 MODIFIED MIX DESIGN

Previous studies have shown the importance of small particle and fine material for cohesion and interlocking behavior, as well as enhance the material loosen over time. Therefore, the PI and percentage passing #200 sieve is increased in the modified mix design. Table 4 illustrates the modified mix design in the last column and also lists the NDOT standard specifications. With the

10% passing #200 sieve and PI at 7, the percentages passing other sieves can be affected slightly. Crush rock is also required to improve cohesion.

Table 4. Modified mix design compared with standard.

Sieve	Crushed Rock for Surfacing (Table 1033.08)	Gravel for Surfacing (Table 1033.07)	Modified NDOT Spec
	Percentage Passing		
1'' (25.0 mm)	100	100	100
¾'' (19.0 mm)			100
½'' (12.5 mm)			
No. 4 (4.75 mm)	40±20	78±17	65±15
No. 8(2.36 mm)			50±15
No. 10 (2.0 mm)	15±15	16	
No. 40 (425 µm)			25±10
No. 200 (75 µm)	5±5	3±3	10
Plastic Index (PI)			7
L.A. Abrasion. Loss, max.	45	40	40
Processing required	Crushed		Crushed

3.4 CONCLUSIONS AND NEXT STEPS

From the results of aggregate sample testing, it was observed that the particles that are passing sieve #200 are critically low in comparison to NDOT modified mixture design specifications, but does meet the current NDOT specifications. To improve the fine material and meet the NDOT modified mixture design, it is decided to mix the existing aggregate with clayey particle prior to the placement on site. Similar to the study carried out by Eggebraaten and Skorseth (2009), a 1-mile gravel roadway in Lancaster County was selected for material placement. The

roadway was planned to be divided into three equal sections (0.33 mile each) for different mixture designs. The three mix designs are quarry deicing mix with 10% clayey material added, county stockpile aggregates (control mix), and quarry deicing mix with 5% clayey material added.

The proposed placement procedures and details are listed below:

- Site Preparation:
    - Properly shape the road first, address drainage problems (driving surface and shoulder drainage), and reshape any washboard regions [1, 2].
    - Remove the previous layer of surface gravel and have the base ready for placement.
    - It is preferred to maintain the same conditions (placement, compaction, thickness, etc.) for the three aggregate mixes (local-typical, local-modified, NDOT-modified) as best as we can.
- Material Placement:
    - Collect representative sets of aggregate samples being placed for laboratory testing-evaluation.
    - The material should be mixed on-site or before placement: it is suggested to have materials blended well as it goes to crusher (do not crush after blending, the graduation needs to be met after crush and blending), or the variations in layers will cause the thickness change or dispense [2]. Note, due to the shrinkage from the materials being placed, 30% or greater reduction in volume [2].
        - Please do this in accordance with “typical mixing.”

        - Careful attention should be made such that any natural clay material to add plasticity and cohesion does not remain in the haul truck boxes. This should be carefully mixed in the gravel.
    - Two inches of the base (rocks) + two inches of surfacing gravel
        - Windrowing the gravel initially is recommended for a well-blended material.

- Procedure:
    - The target crown is 4%. The crown may be eliminated near an intersection (approximately 100-feet transition zone), but the intersection should not be lower to create a location for water ponding. This is done for safety [2].
    - After the material is placed, add moisture only if chloride is applied [1-3].
- Preferences:
    - Compaction is also beneficial, if available. However, this can be omitted if not typically performed (to align with existing procedures). [2]
    - A road closure is preferred, if possible.
- Detailed survey:
    - Limit maintenance activity on roads with tests and monitoring locations.
        - Place signs, if possible.
    - After material placement, the research team will collect a baseline data set for temporal monitoring.

The next step is material order and placement on site. However, due to the project complications, the placement did not occur. It is recommended to trial deploy the modified mix design to understand and quantify the benefit of the modified mix design for Nebraska roads.

CHAPTER 4 – DIGITAL ASSESSMENT

4.1 INTRODUCTION TO PLATFORMS USED

In this project, two remote sensing platforms, including GBL and UAS with an onboard camera as well as georeferenced coordinates data, are used to collect the data. In general and depending on various research demands and equipment available, a UAS with an onboard camera and/or lidar scanner can be implemented as data collection equipment. This chapter initially describes the platforms that are used to collect data and then discusses the assessment procedures and method developed to evaluate the gravel road surfaces.

4.1.1 Lidar Data Collection

The lidar scanners included Faro Focus3D S-350 and Faro Focus3D X-130, as shown in Figures 1a and 1b, respectively. Two scanners were utilized for speed and efficiency in the data collection. The Faro S-350 uses laser class 1 with a wavelength of 1,550 nm and has a maximum range of 1,150 ft. In addition, the S-350 scanner is equipped with a High Dynamic Range (HDR), a high-resolution camera (which can capture images up to 160 MP of resolution) and can collect up to 976,000 points per second with a ranging error of ± 0.07 in and an angular resolution of 0.009˚. The Faro Focus3D X-130 uses a similar laser class. However, the X-130 has a maximum range of 420 ft and can create pictures with a maximum resolution of 70 MP.

(a)

(b)

Figure 1. Lidar platforms used to collect data: (a) Faro Focus3D S-350 LiDAR scanner and (b) Faro Focus3D X-130 LiDAR scanner.

4.1.2 **SfM Data Collection**

The equipment used for the aerial surveys was a DJI Inspire 2 UAS with an onboard Zenmuse X5 camera and mounted 15 mm lens as displayed in Figure 2. Within this UAS platform, the selected flight paths can be autonomously controlled by commercial software while specifying the overlap, flight altitude, and flight speed. Ground sample distance (GSD) which describes how big each pixel is in the resultant dataset. The GSD is a function of flight altitude, image sensor size, and the camera lens field of view. In addition, the GSD can also be set up prior to the UAS data collection step. GSD is considered as the primary factor affecting SfM point cloud density and accuracy.

Figure 2. Remote sensing platform UAS.

4.1.3 GNSS Data Collection

When conducting UAS flights and to obtain accurate georeferenced data within the area of interest, GPS coordinates can be collected at checkboard targets laid out within the surveyed area through Real-Time Kinematic (RTK) surveying process. The accuracy attained by an RTK-GPS survey is usually within 2 to 10 mm. Here the checkerboards can be divided into two classes, including a ground control point (GCP) or checkpoint (CP). A GCP serves as accurate georeferenced GPS information to scale the SfM resultant point cloud to reduce uncertainty while a CP serves as a point to determine the SfM point cloud errors. These known coordinates can be imported prior to point cloud processing to constrain and reduce the point cloud geometry uncertainty. The GCP and CP can also be used within lidar scanning if global accuracy is of importance (true latitude, longitude, and elevation) as well as employed discrete error validation for the CPs.

4.2 DATA COLLECTION STRATEGIES

4.2.1 UAS

The UAS flights are autonomously controlled with the Pix4dcapture, which is an application on a handheld tablet. The flight plans usually contain two flights that are performed for a site with about 85% overlap at an approximately targeted above-ground-level (AGL) altitude of 50 m. Within this project, a forward-facing camera angle of 75° from horizontal is used. This resulted in a computed GSD of 1.11 cm. As shown in Figure 3, the flights covered the area of interest. Note that due to the limited topography at the shown site, a single-grid pattern was conducted. In addition, the ground control points are placed in groups of four targets in approximately 200 m spacing.

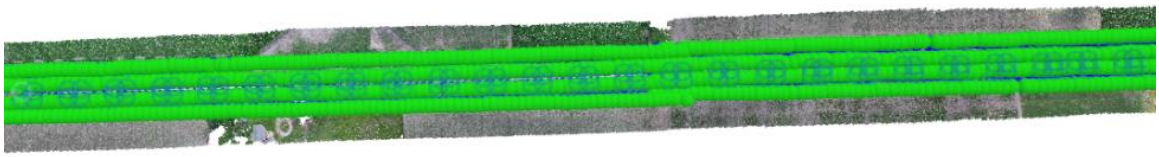

Figure 3. UAS-SfM image locations.

4.2.2 ***Lidar***

To perform the lidar survey, the team used a closed transverse scanning strategy. Within this strategy, a series of scan setups are planned to create a loop, where the first and last scans link together. This allows a reduction in the error propagation during the alignment process. To optimize the lidar data collection process regarding data quality for the time spent at sites, each scan setting is usually set to execute a scan with a point-to-point spacing of 0.3 inches (0.8 cm) at a distance of 10 m, which corresponds to a total of 48 million points per scan within 15 minutes. However, the point density varies depending on the scanner type and scan setup parameters.

The lidar scans were registered using the collected georeferenced coordinates through the RTK-GPS survey technique. The lidar scans were collected with an offset distance of approximately 131 ft (40 m), with four targets per scan location that are used to transfer the collected data to global coordinates. A single-value decomposition (SVD) transformation matrix estimated the coordinate transformation from local coordinates (for each lidar scan) to the global coordinate system. The scan locations are illustrated in Figure 4. These scans were collected with a reduced resolution for time efficiency. The scan setting produced a point-to-point spacing of 0.3 inches (0.8 cm) at a distance of 30 ft (10 m), which corresponds to a total of 9 million points per scan within 5 minutes. The lidar dataset is assumed to be the baseline dataset, given its low mean registration value and its high accuracy internal to each scan (sub-millimeter level).

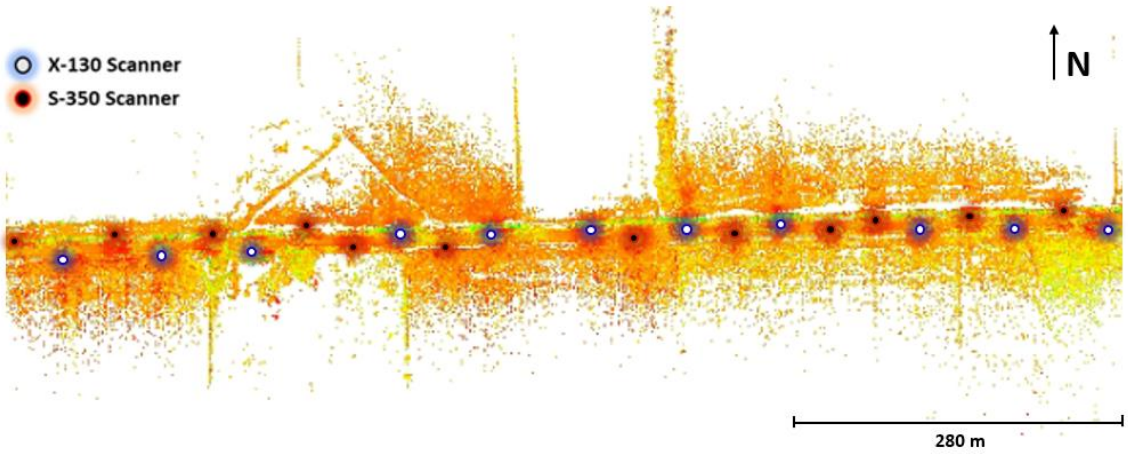

Figure 4. Lidar scan locations and point clouds (colored by intensity).

4.3 SUMMARY OF ALL DATA COLLECTION

UAS and lidar point cloud collection is efficient, requires less workforce than traditional methods, and is less reliant on human biases. UAS acquisition has increased usage of surveying and mapping deployments, for its low-cost, operation ease, and reliable data collection. However, the accuracy is dependent on the quality of images and the georeferenced information. While lidar data collection requires more time in comparison to the UAS data collection process, the level of accuracy for lidar datasets is higher in comparison to UAS derived data. Therefore, the lidar point cloud can be used as a baseline to validate the UAS point cloud errors.

4.4 ERROR ASSESSMENT (UAS VERSUS LIDAR)

Point clouds are a digital representation of a particular object or system of interest in a computer. As a result, a continuous object or system is represented as a collection of points or vertices in a 3D space. The accuracy and the inherent error to the data is a direct function of both the acquisition equipment and the data collection strategy. Since point clouds can be captured from both lidar and UAS-SfM platforms, the error and the quality of the data platforms are

important characteristics to know because they may inhibit or bias the assessment results. Ground control is often time-consuming and cumbersome, but the quantity and distribution of the ground control locations directly influence the error and uncertainty of the data. In addition, both of the lidar and UAS-SfM point clouds are compared to an in-site digital level for validation.

The site of Lancaster County Waverly Street is selected for the error assessment. A 1.6 miles (1 km) section of the selected site is evaluated with various GCP numbers. However, since the focus on this study is road surface assessments, only the hardscape (e.g., gravel roadway surfaces) will be examined in detail. This study assesses the positional errors at discrete locations via checkpoints and as distributed errors throughout the point clouds using the well-cited M3C2 algorithm proposed by Lague et al. 2013. To explore how the number and distribution of ground control points relate to the accuracy and error with UAS SfM point clouds, numerous cases were explored. The numbers of GCPs range from 0 to 22 for the site due to workforce and site accessibility limitations. The comparisons are investigated in both discrete CP errors and distributed quantitative comparisons to lidar point clouds. The distributed error is important to quantify and assess due to the unpredictable errors in SfM point clouds. Here, the study includes extensive distributed error analysis using the M3C2 algorithm and its associated statistical distributions.

The entire scene was aligned using an SVD transformation approach, and its accuracy is directly tied to the RTK-GPS surveying results. For this reason, the error is estimated at approximately 1 to 1.25 inches (2 to 3 cm). The transformed point cloud enables an error assessment at discrete points (CPs) as well as its distribution throughout the site (since lidar data is available). The cases are arranged with an increasing number of GCPs and a decreasing number of CPs, up to a maximum of 22 GCPs. Specifically, case 1 has 96 CPs and 0 GCPs, simulating a

case where no GCP is available nor used. Case 2 has 92 CPs and 4 GCPs only located at the extreme corners on both ends of the site, representing the typically recommended minimum number of GCPs. Case 3 uses GCPs located at the extreme corners and every 1300 ft (400 m), which yields 8 GCPs and 88 CPs. Case 4 contains a total of 12 GCPs located at the extreme corners and in 656 ft (200 m) intervals with 84 CPs. While case 5 uses 18 GCPs located at the extreme corners and in 393 ft (120 m) intervals with 78 CPs. The last case (case 6) utilizes a total of 22 GCPs located at the extreme corners and in 328 ft (100 m) intervals with 74 CPs. This last step simulates a typical case with detailed ground control. Among all six cases, case 6 resulted in the lowest horizontal and vertical errors at the CP locations which are shown in Figure 5.

Lowest horizontal errors

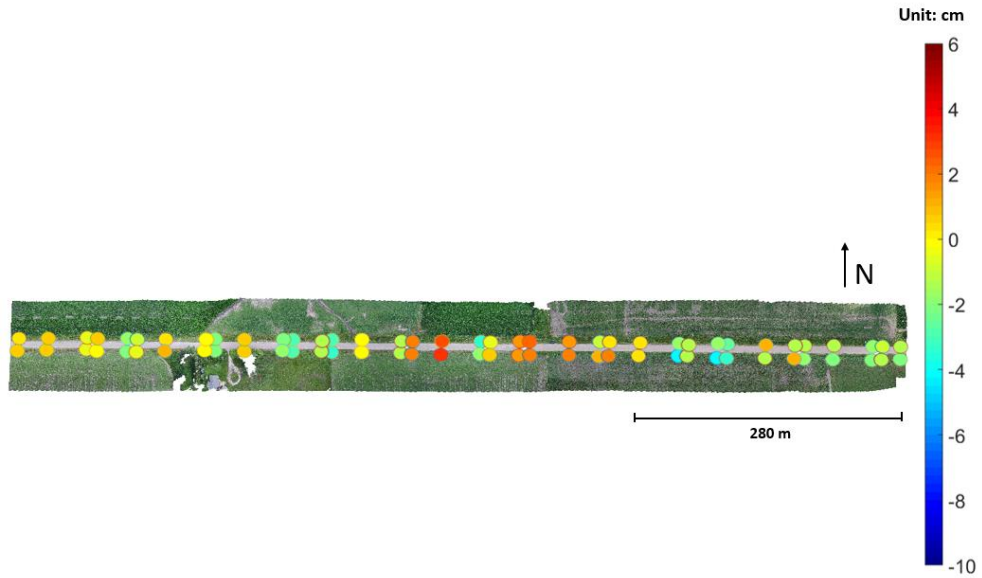

Lowest vertical errors

Figure 5. Horizontal and vertical errors (case with 22 GCPs).

Well distributed GCP locations are a critical parameter for point cloud accuracy, which are used to georeference the UAS photogrammetric data. Investigating the most accurate and efficient GCP layout distribution is essential in SfM applications. Figure 6 depicts the absolute horizontal errors for the mean 50%, 68%, and 95% intervals comparison for each case against the number of GCPs. The general trend demonstrates that as the number of GCPs increases, the errors decrease. Moreover, it can be observed that case 6 has the lowest and conservative vertical errors. It is indicated that case 6 has the highest accuracy in the study when considering the 95% confidence level, which is typically the norm in the assessment of geospatial errors.

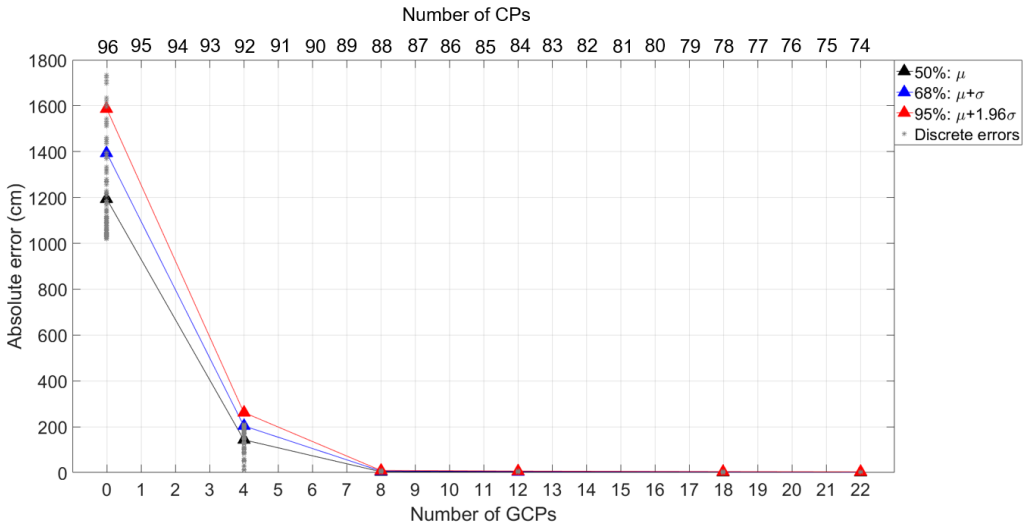

(a) Cases 1-6

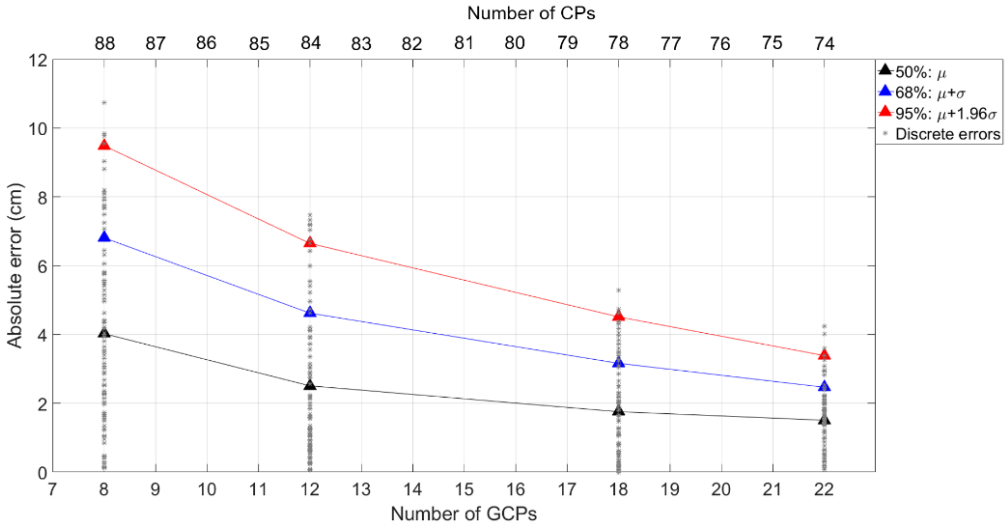

(b) Cases 3-6

Figure 6. Discrete errors.

The overall accuracy and quality of the point cloud datasets, as well as the assessment output, are critical for reliable analysis and deliverables. Consequently, both point clouds and assessment parameters will be validated to known dimensions or the in-site assessment results. This validation will be quantitatively computed for reliability and feasibility purposes. In detail, for the gravel road assessments, the validation includes the geometry comparison to the in-site

measurements, which includes the roadway widths, slopes, and other measured distances within the site.

For example, a validation in terms of the gravel road section is extracted as shown in Figure 7. The two extracted cross-sections on the gravel roadway are compared to onsite slope measurement using a digital level. These two cross-sections are not compared to a design manual since gravel roads can degrade quickly due to environmental and traffic loads. An external verification was performed using a digital level, which was placed on a 3.2 ft (1 m) straight edge with a specified accuracy of 0.05° with a precision of one-tenth of a percent. The digital level provided measurements of 4.0% and 3.3% at sections C-C and D-D, respectively. The point clouds of these sections are shown in Figure 8. The crown geometry analysis results of the selected sections are also presented in Table 5. Both lidar and SfM point clouds have slope values that are similar to onsite measurements of 4.0% and 3.3%, respectively. Note that these measurements will only be close since the digital level did not represent the entire lane width, but the largest difference is only 8% for the SfM slope at D-D. These values indicate that both datasets are similar and close to the measured values with an average difference of 3%. As a result, the point clouds and slope assessment is validated to be reliable and accurate.

Figure 7. Extracted sections for QA/QC validation.

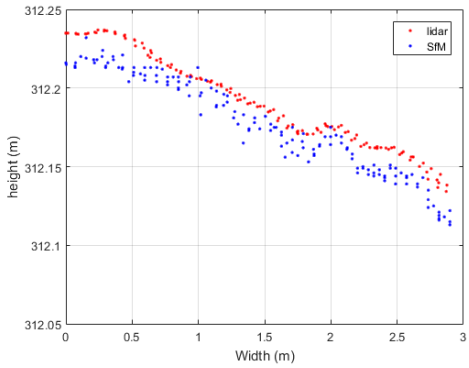

Point clouds at section C-C

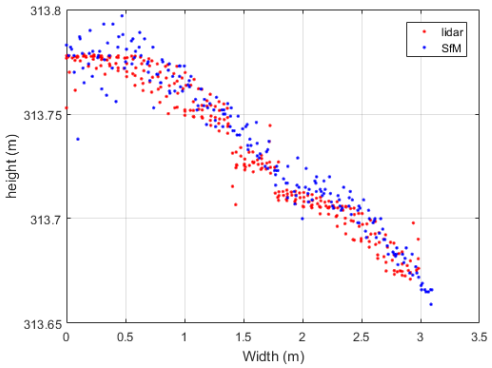

Point clouds at section D-D

Figure 8. Cross-section view at the extracted sections.

Table 5. Slope comparisons at extracted sections.

Section	Calculated Slope (%)		Digital Level Measurement (%)
	Lidar	SfM	
C-C	4.08	4.12	4.0
D-D	3.36	3.58	3.3

4.5 ASSESSMENT PROCEDURES

The first step of processing techniques is the coordinate transformation. This is computed for points of the point cloud and then applied a best-fit plane. This step is included in the process because the surface does not remain flat or level. Consequently, the elevation and direction changes, which is undesired. The second step is the segmentation process in which slices at each desired location are extracted along the user-defined length of the point cloud. Within this procedure, slices at each segment are extracted at uniform intervals for representation along the length in terms of point cloud cross-section. In addition, the slice thickness and segment width of each profile can be configured. For instance, the slices are typically defined as 0.3 to 1.6 ft (0.1 to 0.5 m) in width and a segmentation distance of 16 to 65 ft (5 to 20 m). These parameters are dependent on the density of point cloud that is being analyzed.

The next process is a low-pass filter to remove the inherent noise in the point cloud in the point cloud. Noise in point cloud can be caused by beam divergence, moving objects in the collected data (i.e. vehicles and pedestrians), reflective surfaces (i.e., wet surfaces, glass or mirrorlike objects), and undesirable data present in the environment (i.e., vegetation). A low-pass filter removes any inherent noise and therefore smooths the point cloud extracted profiles. This filter will conduct a moving average over each segment using a user-defined span width. For example, the span width can vary from 20 to 80 points, depending on the density of the segmented point cloud. An example of the low-pass filter is illustrated in Figure 9.

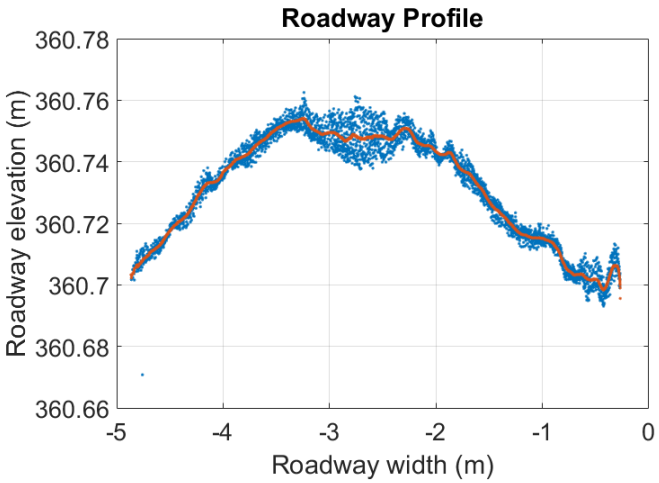

Figure 9. Segmentation and low pass filter.

The next step in the process is to identify the best fit curve for the segmented profiles. The aim of the curve fitting process is to attain objective geometric parameters. A second-order polynomial is fitted to each profile, where this shape is selected due to the best fit via regression. An example is displayed in Figure 10a. Note a second-order polynomial is chosen given its general shape for a roadway with a crown. With the completion of the fitted curve for each segment, the central point can be located automatically, and then the corresponding crown slopes are computed (Figure 10b). Curve fitting is performed to objectively determine the center location of the crown

profile, since this may be multi-peaked due to rutting and other undesirable degrading behavior of gravel aggregates. The crown slopes are also known as cross-sectional slopes, which for gravel road should be near the target of 4% (Federal Highway Administration 2015).

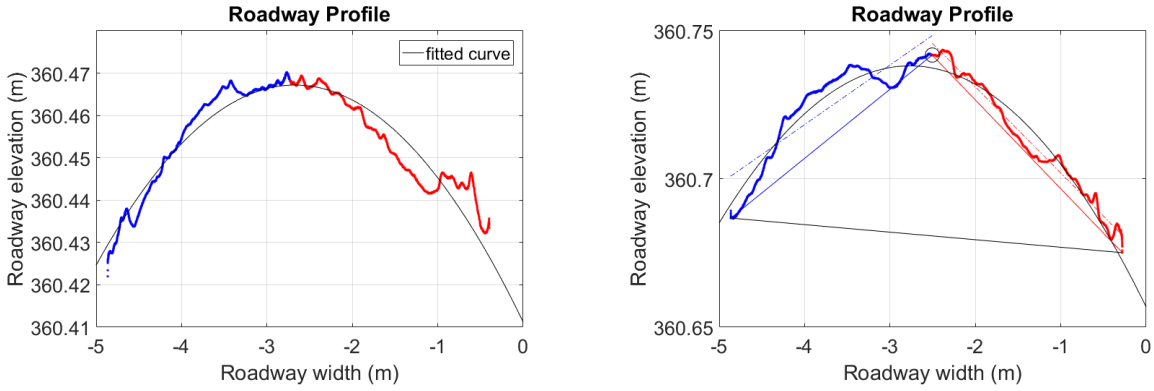

Figure 10. Gravel road profiles: (a) second-order curve fitted to the point cloud and (b) computed cross slope for each side of the extracted profile.

*4.6 **RESULTS AND DISCUSSION***

The gravel road performance consistency is evaluated in terms of the width, elevation change within each segment, and the crown slopes. An example of a gravel road located at N 162nd street within Waverly Rd. to Bluff Rd, which is a 1-mile (1.6 km) section without intersection or significant elevation change. Data collection was carried out on April 22, 2018, and July 13, 2018, where no maintenance was performed between the two assessment stages. Therefore, the comparison of width along the roadway, elevation change within segmentation, and crown slopes are due to natural degradation from the environment and vehicular loads (Figure 11).

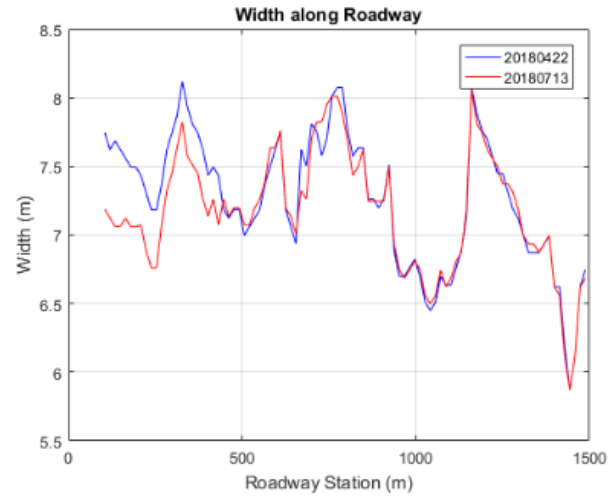

(a)

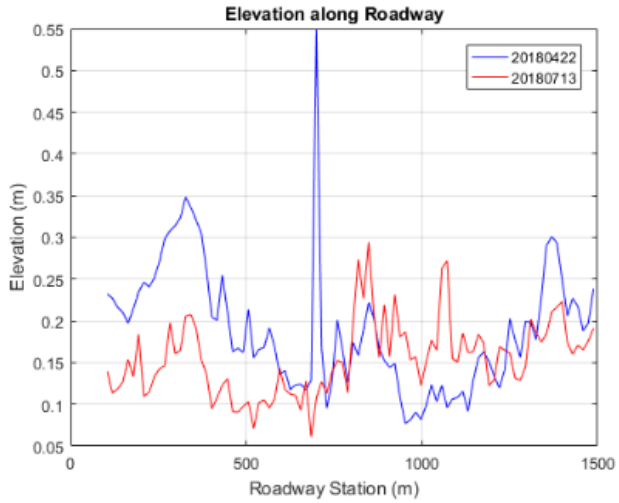

(b)

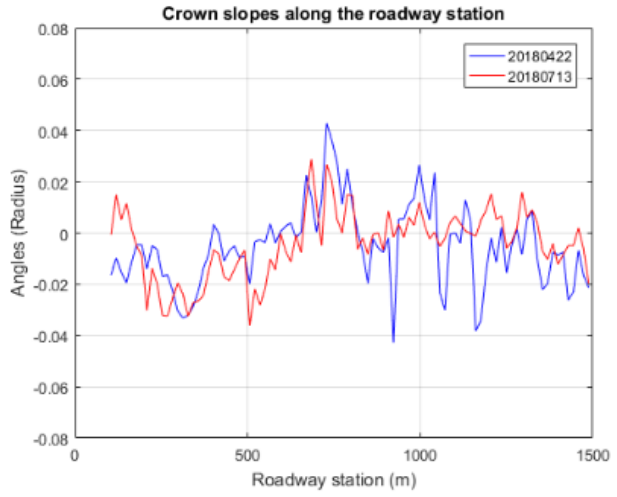

(c)

Figure 11. Comparison of two datasets: (a) width, (b) elevation change, and (c) crown slopes.

It can be concluded that the gravel road has similar widths for both datasets, but reduced elevation (per segmentation) and cross-sectional slopes, which was expected since no maintenance was performed. For the ease of the overall assessment visualization, cloud-to-cloud distance measurement, and surface roughness can also be computed. Datasets collected at various times can be compared to estimate cloud-to-cloud distance using M3C2 function in CloudCompare software, which computes the changes between two point clouds. The cloud-to-cloud distance results directly show the horizontal and vertical deformation with time changes. The collected two datasets are compared using the M3C2 function (Figure 12). As for roadway roughness estimation, it is computed in CloudCompare software between the points and the best-fitting plane. The surface geometry can be detailed shown by roughness, including tire tracks (Figure 13). While the cloud-to-cloud and the surface roughness can illustrate degradation of the roadway, these results are not considered directly in the objective assessment strategy.

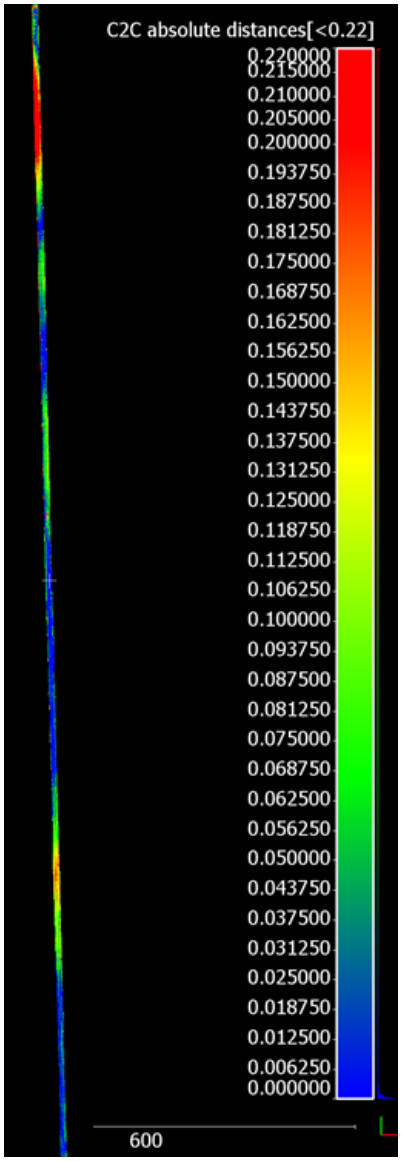

Figure 12. Cloud to cloud distance results of the two datasets.

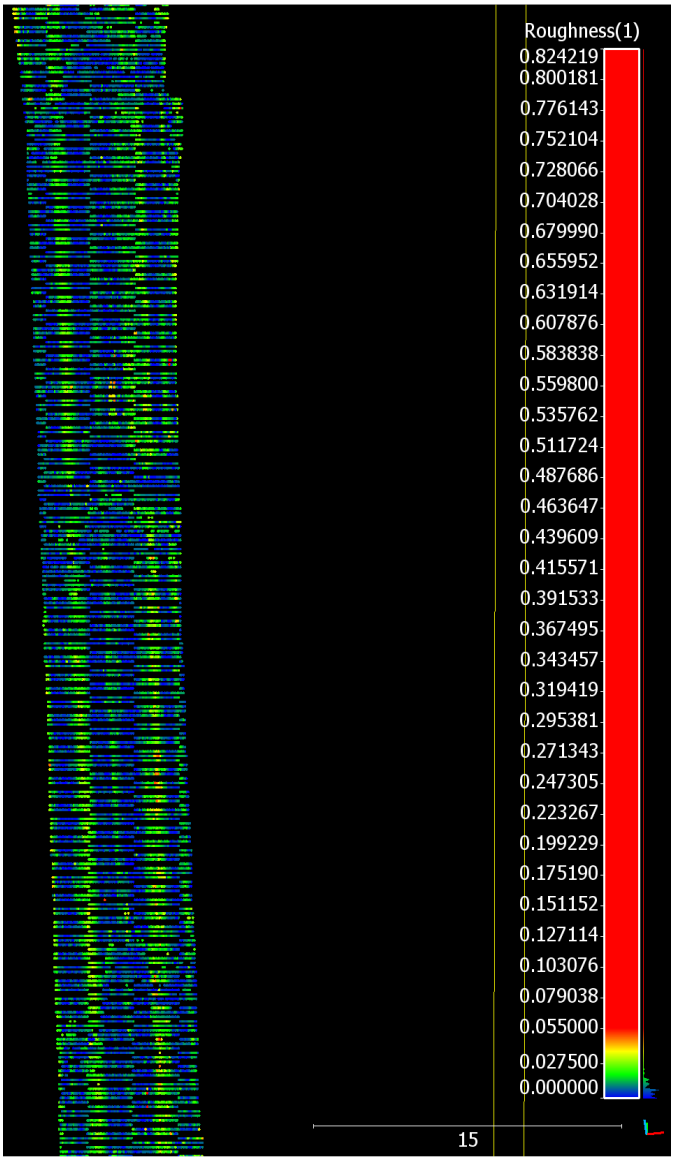

Figure 13. Surface roughness.

To further substantiate the assessment of the roadway's conditions for the decision-making process, various statistical parameters are computed. These parameters include mean(μ), standard deviation (σ), and coefficient of variation (COV), as illustrated in Table 6. The positive and negative slope mean values are slightly higher than 4%, especially the negative values with a mean value of 4.80%. However, the standard deviation and coefficient of variation indicate a more

significant spread in the data than desired. This highlights that while on average, this roadway has approximately 4% slope grade, actual slope values vary significantly – indicating its reduced travel safety and drainage. Decision making based on the mean and its probability distribution is possible to rate the conditions of the roadway and optimize maintenance schedules.

Table 6. Statistical parameters of crown slopes along the roadway.

Slope Values	**μ (%)**		**σ (%)**		**COV**	
	Positive	**Negative**	**Positive**	**Negative**	**Positive**	**Negative**
20180422	4.31	3.79	1.21	0.99	0.29	0.39
20180713	3.88	2.56	2.72	1.47	0.70	0.39

4.7 CONCLUSIONS

As described in previous sections, the developed method can analyze roadway surface point clouds from lidar scanners or UAS SfM platforms and assess the geometry of the road profile. Point clouds obtained from gravel roadways through lidar scanners and UAS SfM can accurately characterize the roadway's performance for long or short-term monitoring applications and used as key information for decision-making processes if maintenance or rehabilitation operations are required. Furthermore, the developed method analyzes the depth map of the roadway to characterize the performance of the surface for defects such as potholes.

CHAPTER 5 - CONCLUSIONS

5.1 INTRODUCTION

The field of civil engineering is increasing using emerging infrastructure assessment techniques that rely on point clouds. Traditionally, gravel road performance assessment is commonly performed using onsite measurement and observations by instruments such as measuring tapes, straight edges, levels, or total stations. These methods are time-consuming, inefficient, and results can be subjective, which may produce drastically different assessments and characterizations due to slight variations in placements. Therefore, an advanced method in this manuscript is proposed to assess the gravel road from 3D point cloud data. Point clouds can be collected with increased accuracy and cost and time-efficient approaches.

5.2 KEY FINDINGS

Within the evaluation, crown profiles and overall performance metrics are the essential evaluation factors for temporal assessments. In this approach, the accuracy of the developed methodology is within the sub-inch or centimeter-level, which is adequate for the specific assessment applications. Quantifying the data include parameters such as segmentation width and its intervals and filter span width that can be adjusted for various point cloud density and output deliverables.

This methodology can automatically and objectively assess gravel roadway surfaces based on 3D point clouds. The point clouds obtained from both lidar scanners and UAS derived SfM can accurately characterize the condition of the gravel roadways and provide vital information that can be used for the decision-making process. The proposed assessment uses geometric feature

mining and statistical processing concepts. Moreover, the remote sensing data collection is efficient, required less workforce than traditional methods, and does not rely on inspector/human biases.

5.3 USE OF DIGITAL ASSESSMENT IN OTHER TRANSPORTATION APPLICATIONS

The application and usage of remote sensing technology have increased in recent years within all fields of civil engineering, in particular, transportation engineering. Remotely sensed three-dimensional point clouds have a high potential for various assessment applications, including but not limited to structural damage detection and quantification, geotechnical evaluations such as slope stability and rockfall analyses, and transportation-related applications such as asset management and asset inventories (Liao et al. 2019). The following sections aim to highlight the potential application of point cloud data for the assessment of transportation-related infrastructure. As demonstrated, the implementation of lidar data can improve and ultimately transform the way in which transportation agencies assess and maintain the transportation-related infrastructure.

5.3.1 Structural Damage Detection, Quantification, and Deformation Analysis

Structural damage detection and quantification is one of the early implementations of remotely sensed data for digital assessment. Specifically, the lidar derived point clouds have been used to develop a series of automated damage detection methods to locate and quantify damaged areas. Within transportation infrastructure, these methods focused on assessing bridge piers, girders, abutments, guard rails, deck conditions, and barriers for various damage types, defects, and other anomalies. However, as lidar derived point clouds can only capture and represent the surface objects, the developed damage detection and quantification methods can identify the

damage types that are evident based on color variation or geometric changes including but not limited to cracking, spalling, corrosion, and loss of cross-sections. The damage detection methods can be classified into two general categories, including methods that rely on capturing temporal changes between two datasets of identical objects and studies that use nontemporal datasets to detect damage (without relying on change detection). While the methods that developed based on temporal changes, such as Olsen (2015) compare two datasets of the same object collected in different times to capture changes (i.e., damaged areas), the developed damage detection methods based on nontemporal approach such as Mohammadi et al. (2019), Vetrival et al. (2018), Valenca et al. (2017), Erkal and Hajjar (2017), and Kashani et al. (2015), locate and quantify the damaged areas by analyzing various geometric and spectral features of each point within the point cloud dataset (Figure 14). These algorithms utilize various clustering algorithms, nonparametric statistical analysis methods, or maternal learning techniques to detect the location of likely damaged areas. Irrespective of the developed methods, these developed methods can reduce the cost and time of evaluation, improve accuracy, and ultimately reduce subjectivity that is associated with visual inspections conducted for damage assessments.

(a) (b) (c) (d)

Figure 14. Example of damage detection from in a point cloud of a bridge pier: (a) image of bridge prier along with observed defects, (b) RBG colored point cloud, (c) the color-coded point cloud data were color red (grey color in black and white versions) represents the detected potentially damaged areas, and (d) classification of identified damaged areas based on severity (courtesy of Mohammadi et al. 2019).

Bridges are one of the vital transportation structures, and therefore various method exists to monitor bridges under various loads including static, quasi-static, and dynamic loads. One of the most accurate methods to perform deformation monitoring is performed based on remotely sensed point clouds, which allows to monitor deformation measurements under static, quasi-static, and more recently dynamic loading conditions (Park et al. 2007; Wood 2014; Jatmiko and Psimoulis 2017; Martindale et al. 2019; Watson 2019). The deformation analysis processes, similar to damage detection and quantification methods, can be performed based on either change detection analysis similar as demonstrated by Martindale et al. (2019) and Watson (2019) or using a single dataset of the bridge (Park et al. 2007; Wood 2014; Jatmiko and Psimoulis 2017).

*5.3.2 **Geotechnical Characterization and Assessment***

Point clouds are also used for various geotechnical site characterization and assessments, including slope and embankment stability, landslides, and rockfall analysis, in particular, for the areas within the proxy of roads and highways. Within these assessments and similar to damage detection methods from point clouds, the two approaches were used, including studies that used change detection and studies that used single datasets that do not rely on temporal changes. The change detection methods are predominately used for monitoring and documenting areas that are susceptible to changes included coastal areas, embankment, landslides, and slope stabilities (e.g., Olsen 2015; Sharifi-Mood 2017). Figure 15 illustrates an example case study of change detection for slope stability analysis. Within this case study, a change detection algorithm quantifies the changes within the region of interest due to slope failure for the span of 8 months.

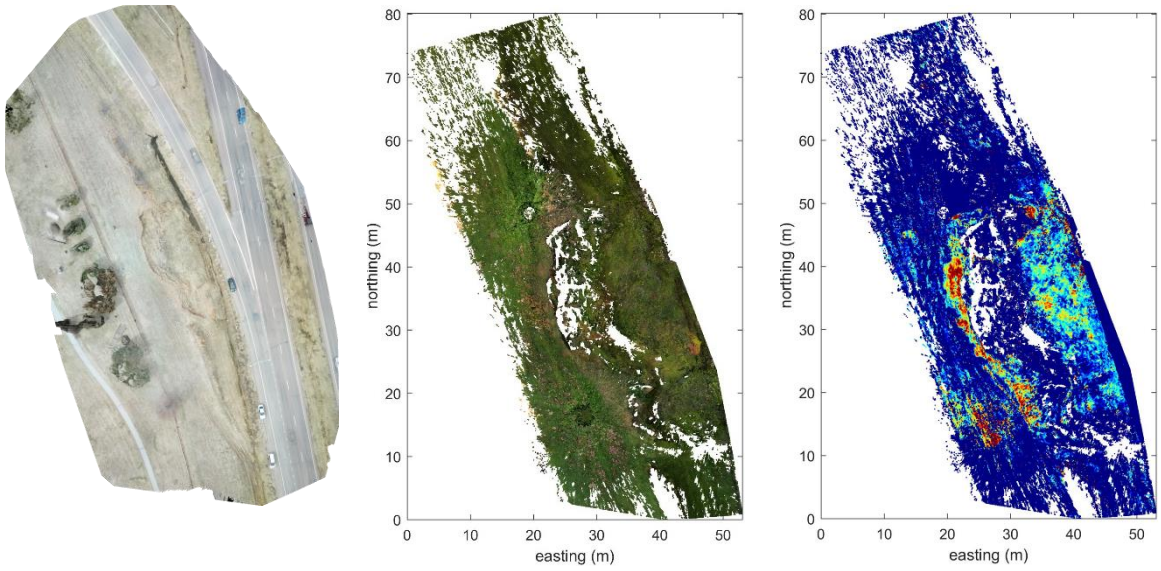

(a) (b) (c)

Figure 15. The slope stability analysis base on the change detection for a region, located in the southeast of I-180, Lincoln, NE, sustained slope failure. (a) aerial image of the site, (b) RGB colored point cloud, and (c) color-coded point cloud were different colors represent different levels of changes (Song et al. 2018).

In addition to the change detection method, various studies have also used a single point cloud dataset for the task of geotechnical assessment. Within this approach, initially, one or a series of features that describe the underlying geometry of the point cloud data are identified. Afterward, the points within the dataset are classified based on a series of conditions or an index. For example, Dunham et al. (2017) introduced a method to assess rockfall hazards via point cloud data by establishing a Rockfall Activity Index. Within this study, Dunham et al. (2017) initially arranged the points within the dataset into cells and then computed a geometric descriptor (here a normal vector) for each cell. Through the normal vector orientation in the three-dimensional space, the surface of the rock was then classified into 7 categories based on their topographic style and geometric expressions.

*5.3.3 **Other Areas***

Due to the efficiency of remote sensing platforms in collecting point cloud data in terms of accuracy, precision, and rate of data collection, the point clouds can be used in a wide range of applications besides structural and geotechnical assessments. These applications include the assessment of highways as well as extracting roadside and on-road information from point clouds. This section provides a summary of the most common applications of point clouds for highway assessments, asset inventories and management, and roadway design and geometry analyses. The point cloud data collected from the roads and highways contain various items other than objects of interest (e.g., road signs, lane marking, road surface). As a result, the primary process that is shared with the majority of the applications developed for highway assessments, asset inventories and management, and roadway design and geometry analyses are to detect and extract the objects or areas of interest from the point clouds.

Various studies, such as Lam et al. (2020) and Wang et al. (2012), proposed algorithms to isolate and extract road surfaces from lidar data for condition assessment of road surfaces. Extracted pavement point clouds can be used in the evaluation of the road surfaces, including lane markings and pavement conditions (Kodagoda et al. 2006; Grafe 2008; Zhang 2010). The extracted road surface point cloud can be used to create accurate and detailed mesh models of the pavement, or the lane markings can be evaluated based on the reflectivity for wear and tear. In addition, the traffic signs and signals can be detected and identified from point clouds based on their locations and unique geometries, which not only facilitates the condition assessment of these objects but also it provides an efficient method to update the traffic signs inventory and the locations (e.g., Vu et al. 2013). Similar to traffic signs, other roadside objects including lamp posts, trees, power lines, and other utility poles and objects, can be mined from road and highway point clouds. In particular, these data can provide the department of transportations an efficient option to document the location, count, type, and current condition of the objects that are existed on roadsides (e.g., Lehtomaki et al. 2011). Lastly, the collected point clouds can be used for various geometric analyses, including cross-section orientation evaluations, vertical alignments, and site distance assessments. These point clouds can be used to creating as-built models of roads and highways to study the drainage performance, lateral clearances, and curved slopes (Tsai et al. 2011). In addition, traffic signs, roadside objects, and other highway features may change due to construction, excavation, or pavement maintenance operations, which can affect the initial sight distances (e.g., Castro et al. 2016). As a result, the sight distances can also be evaluated and for safety applications and inform future retrofit projects.

*5.4 **FUTURE WORK***

This assessment methodology using 3D point clouds, which can be further developed into general procedures and specific applications for various infrastructure or other systems. It can be automatically processed with the input of point clouds containing XYZ coordinates, intensity, and RGB color information. The output files can be platforms of figures, matrix arrays, colorized point cloud, etc. Moreover, the modified mix design is expected to improve the gravel road performance substantially, which was the initial goal of the project. This mix design can be placed and assessed in the future for further evaluation using the developed algorithms from this project with relative ease.

REFERENCES

Baiqi, L., Jianli, L., and Taizhong, K. (2011). An SINS/GPS/odometer integrated navigation system for profile measurement. *Proc. in IEEE 10th International Conference on Electronic Measurement & Instruments*, IEEE, Chengdu, China, 1, pp. 45-48.

Brooks, C., Dobson, R. J., Banach, D., Dean, D., Oommen, T., Wolf, R.,E., Havens, T.,C., Ahlborn, T., M., and Hart, B. (2015). Evaluating the use of unmanned aerial vehicles for transportation purposes. Report No. RC-1616, Michigan Department of Transportation, Lansing, MI, USA.

Castro, M., Anta, J.A., Iglesias, L., and Sánchez, J.A. (2014). GIS-based system for sight distance analysis of highways. *J. Comput. Civil Eng.*, 28(3), 04014005.

Dobson, R.J., Brooks, C., Roussi, C., and Colling, T. (2013). Developing an unpaved road assessment system for practical deployment with high-resolution optical data collection using a helicopter UAV. *Proc. in 2013 International Conference on Unmanned Aircraft Systems (ICUAS)*, IEEE, Atlanta, GA, pp. 235-243.

Eggebraaten, T. and Skorseth, K. (2009). SDDOT/SDLTAP Gravel Road Experimental Project. United States Department of Transportation, Pierre, SD.

Erkal, B.G., and Hajjar, J.F. (2017). Laser-based surface damage detection and quantification using predicted surface properties. *Automat. Constr*., 83, 285-302.

Federal Highway Administration (FHWA) (2015). *Crown. Gravel Roads Construction & Maintenance Guide*, Publication No.: FHWA-OTS- 15-0002, United States Department of Transportation, Brookings, SD.

Fernandez Galarreta, J., Kerle, N., and Gerke, M. (2015). UAV-based urban structural damage assessment using object-based image analysis and semantic reasoning. *Nat. Hazard Earth Sys*, 15(6).

Giesko, T., Zbrowski, A., and Czajka, P. (2007). Laser profilometers for surface inspection and profile measurement. *Probl. Ekspl.*, 97-108.

Gräfe, G. (2008). Kinematic 3D laser scanning for road or railway construction surveys. *Proc. in of the International Conference on Machine Control & Guidance*, Zurich, Switzerland, pp. 24-26.

Jatmiko, and Psimoulis, P. (2017). Deformation monitoring of a steel structure using 3D terrestrial laser scanner (TLS). *Proc. in: 24th EG-ICE International Workshop on Intelligent Computing in Engineering*, Nottingham, UK,10-12.

Kashani, A.G., M. J. Olsen, and Graettinger., A.J. (2015). Laser scanning intensity analysis for automated building wind damage detection. *Proc., International Workshop on Computing in Civil Engineering*, ASCE, Austin, TX, 199-205.

Kodagoda, K., Wijesoma, W.S., and Balasuriya., A.P. (2006). CuTE: Curb tracking and estimation. *IEEE Trans. Control Syst. Technol.*, 14(5), 951- 957.

Lague, D., Brodu, N., and Leroux, J. (2013). Accurate 3D comparison of complex topography with terrestrial laser scanner: Application to the Rangitikei canyon (NZ). *ISPRS J Photogramm.*, 82, pp.10-26.

Lam, J., Kusevic, K., Mrstik, P., Harrap, R., and Greenspan., M. (2010). Urban scene extraction from mobile ground based lidar data. *Proc.in 5th International Symposium on 3D Data Processing, Visualization, and Transmission, 3DPVT*, Paris, France, pp. 1-8.

Lee, J.H., Lee, S.H., Kang, D.K., Na, S.D., and Yoo, W.S. (2017). Development of a 3D road profile measuring system for unpaved road severity analysis. Int. J. Precis. Eng. Man., 18(2), pp.155-162.

Lehtomäki, M., Jaakkola, A., Hyyppä, J., Kukko, A., and Kaartinen, H. (2011). Performance analysis of a pole and tree trunk detection method for mobile laser scanning data. *Int. Arch. Photogramm. Remote Sens. Spat. Inf. Sci*., 38, 197-202.

Liao, Y., Mohammadi, M.E., Watson, P.E., Wood, R.L., Song C.R., Kim, Y.R. (2019). Applications of LiDAR for SDDOT, Report No. SD2013-10-F, South Dakota Department of Transportation, Pierre, SD.

Mohammadi, M.E., Wood, R.L., and Wittich, C.E. (2019) Non-Temporal Point Cloud Analysis for Surface Damage in Civil Structures. *ISPRS Int. J. Geo-Inf*., 8, 527.

Martindale, G., Watson, D., Kodsy, A. M. K. M., El-Khier, M. A., Wood, R. L., and Morcous, G. (2019). Performance evaluation of inverted tee (IT) bridge system, Report No. 2611214037-001, Nebraska Department of Transportation, Lincoln, NE.

Nebraska Department of Roads (2007). “Aggregates”, Standard Specifications for Highway Construction, Nebraska Department of Roads, Lincoln, NE.

Olsen, M. J. (2015). In situ change analysis and monitoring through terrestrial laser scanning. *J. Comput. Civ. Eng*., 29(2), 04014040.

Sharifi-Mood, M., Olsen, M. J., Gillins, D. T., and Mahalingam, R. (2017). Performance-based, seismically-induced landslide hazard mapping of Western Oregon. *Soil Dyn Earthq. Eng*., 103, 38-54.

Smith, J., Hunter, K.P., and Booker, T. (2000). Gravel roads maintenance and design manual. South Dakota Local Transportation Assistance Program (LTAP), United States Department of Transportation, Pierre, SD.

Song, C., Wood, R.L., Wittich, C.E. (2018). Identification of Slope Movement Based on Surface Lidar and Surface Imagery Techniques. 53rd Annual Shallow Exploration Drillers Clinic, La Vista, Nebraska, April.

South Dakota Department of Transportation (2015). Aggregates for granular bases and surfacing. Specifications for Roads and Bridges, South Dakota Department of Transportation, Pierre, SD.

Tsai, Y., Yang, Q., and Wu, Y. (2011). Use of light detection and ranging data to identify and quantify intersection obstruction and its severity. *Transport. Res. Rec.*, 2241(1), 99-108.

Transportation Information Exchange (1984). Soils for road work, Report No. 05404, Saint Michael's College, Winooski, VT.

Valença, J., Puente, I., Júlio, E., González-Jorge, H., and Arias-Sánchez, P. (2017). Assessment of cracks on concrete bridges using image processing supported by laser scanning survey. *Constr. Build Mater*., 146, 668-678.

Vu, A., Q. Yang, J. A. Farrell, and Barth., M. (2013). Traffic sign detection, state estimation, and identification using onboard sensors. *Proc. in 16th International IEEE Conference on Intelligent Transportation Systems (ITSC 2013)*, IEEE, Hague, Netherlands, pp. 875-880.

Vetrivel, A., Gerke, M., Kerle, N., Nex, F., and Vosselman, G. (2018). Disaster damage detection through synergistic use of deep learning and 3D point cloud features derived from very high resolution oblique aerial images, and multiple-kernel-learning. *ISPRS J. Photogramm.*, 140, 45-59.

Wang, H., Z. Cai, H. Luo, C. Wang, P. Li, W. Yang, S. Ren, and Li., J. (2012). Automatic road extraction from mobile laser scanning data. *Proc. in Computer Vision in Remote Sensing (CVRS)*, IEEE, Xiamen, China, pp. 136-139.

Watson, D.P. (2019). Lidar assessment to monitor bridge response under live and dead loads. Master Thesis, Department of Civil and Environmental Engineering, University of Nebraska-Lincoln, Lincoln, NE, USA.

Williams, K., Olsen, M. J., Roe, G. V., and Glennie, C. (2013). Synthesis of transportation applications of mobile LiDAR. *Int. J. Remote Sens.*, 5(9), 4652-4692.

Wood, R.L. (2014). Methods of structural damage characterization for infrastructure. *Proc. of 34th Annual Structural Congress*. Structural Engineering Association of Nebraska, Omaha, NE, 12pp.

Yang, J.S., Goo, S.H., Bae, C.H., and Lee, S.H. (2007). Development of profilometer for profile measurement and severity analysis of unpaved test courses. *J. Korean Soc. Precis. Eng.*, 24(1), pp.37-46.

Zhang, W. (2010). LIDAR-based road and road-edge detection. *Proc. in Intelligent Vehicles Symposium (IV)*, IEEE, San Francisco, CA, pp. 845-848.

APPENDIX A

Figure 16. Location of Waverly St in Lancaster County.

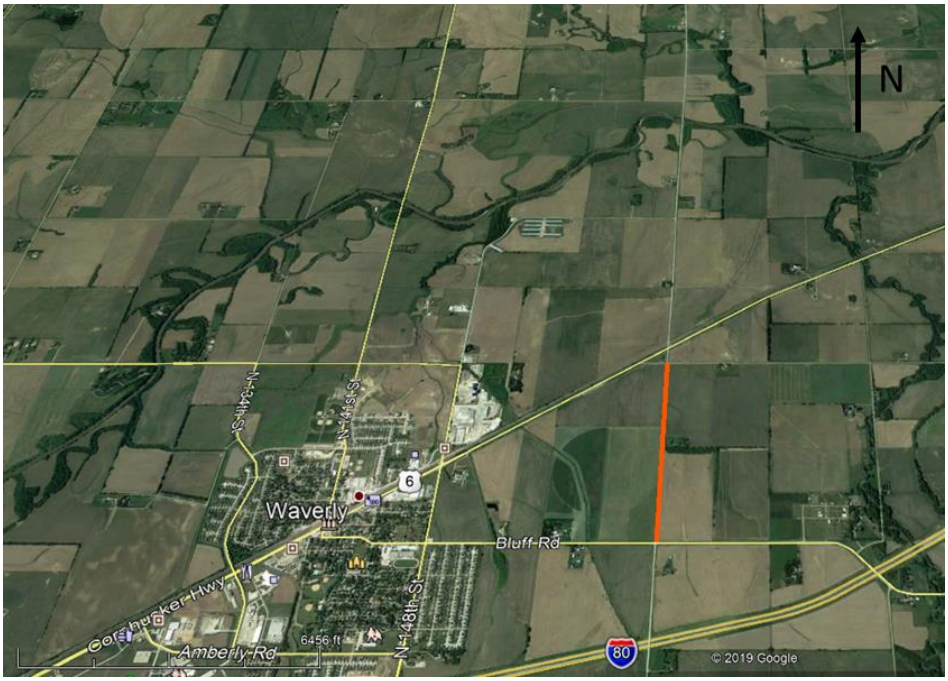

Figure 17. Location of N 162nd St in Lancaster County.

Figure 18. Location of 1900 St. in Saline County.

Figure 19. Location of 2300 St. in Saline County.

Table 7. Data collection parameters for Waverly St. in Lancaster County on August 30, 2018.

Number of flights	Number of Images	Flight Altitude	Ground Sample Distance (GSD)
2	797	161 ft 49 m	0.42 inch 1.07 cm

Table 8. Data collection parameters for Waverly St. in Lancaster County on December 15, 2018.

Number of flights	Number of Images	Flight Altitude	Ground Sample Distance (GSD)
2	1002	154 ft 47 m	0.40 inch 1.03 cm

Table 9. Data collection parameters for Waverly St. in Lancaster County on March 21, 2019.

Number of flights	Number of Images	Flight Altitude	Ground Sample Distance (GSD)
4	1073	156 ft 47.5 m	0.41 inch 1.04 cm

Table 10. Data collection parameters for N 162nd St. in Lancaster County on April 22, 2018.

Number of flights	Number of Images	Flight Altitude	Ground Sample Distance (GSD)
2	654	148 ft 45 m	0.39 inch 1.00 cm

Table 11. Data collection parameters for N 162nd St. in Lancaster County on July 13, 2018.

Number of flights	Number of Images	Flight Altitude	Ground Sample Distance (GSD)
3	1054	159 ft 48.5 m	0.42 inch 1.06 cm

Table 12. Data collection parameters for 1900 St. in Saline County on February 27, 2018.

Number of flights	Number of Images	Flight Altitude	Ground Sample Distance (GSD)
2	429	192 ft 58.5 m	0.5 inch 1.28 cm

Table 13. Data collection parameters for 1900 St. in Saline County on April 4, 2018.

Number of flights	Number of Images	Flight Altitude	Ground Sample Distance (GSD)
1	401	143 ft 43.5 m	0.38 inch 0.95 cm

Table 14. Data collection parameters for 2300 St. in Saline County on April 5, 2018.

Number of flights	Number of Images	Flight Altitude	Ground Sample Distance (GSD)
2	826	148 ft 45 m	0.39 inch 0.98 cm

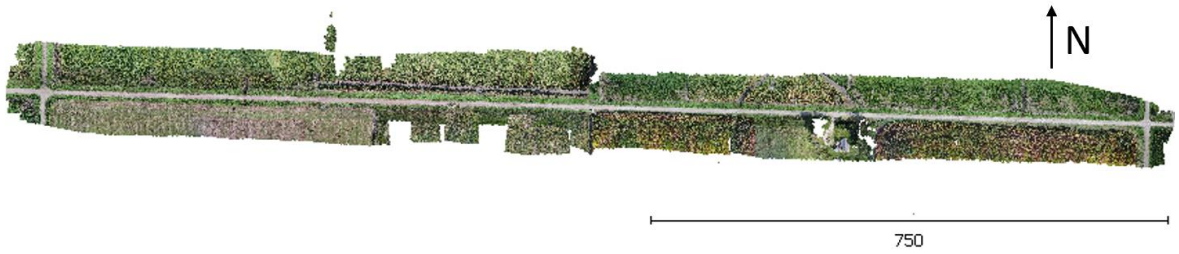

Figure 20. Processed UAS SfM collected on August 30, 2018 of Waverly St. in Lancaster County (scale in meters).

Figure 21. Processed UAS SfM collected on December 15, 2018 of Waverly St. in Lancaster County (scale in meters).

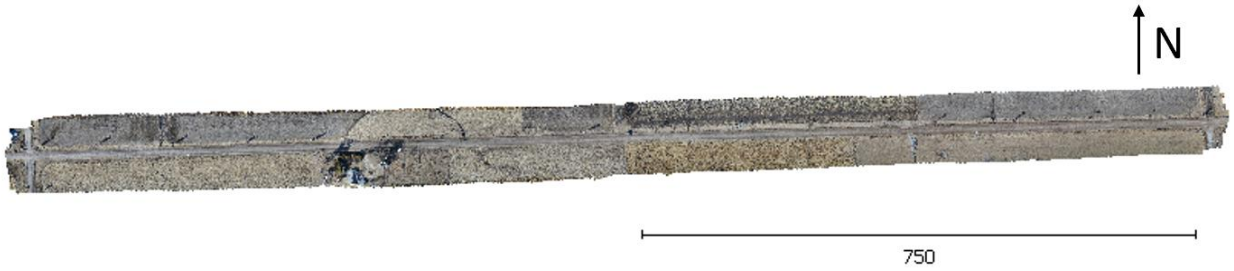

Figure 22. Processed UAS SfM collected on March 21, 2019 of Waverly St. in Lancaster County (scale in meters).

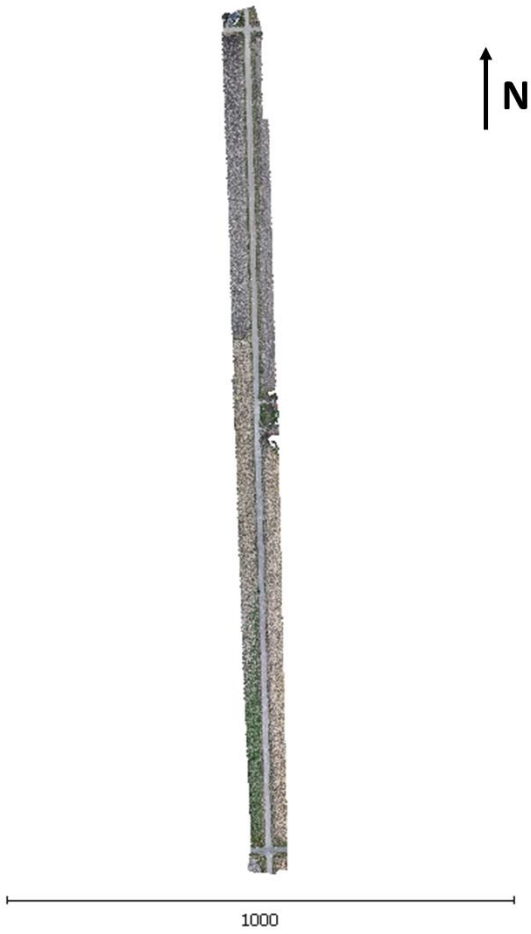

Figure 23. Processed UAS SfM collected on April 22, 2018 of N 162nd St. in Lancaster County (scale in meters).

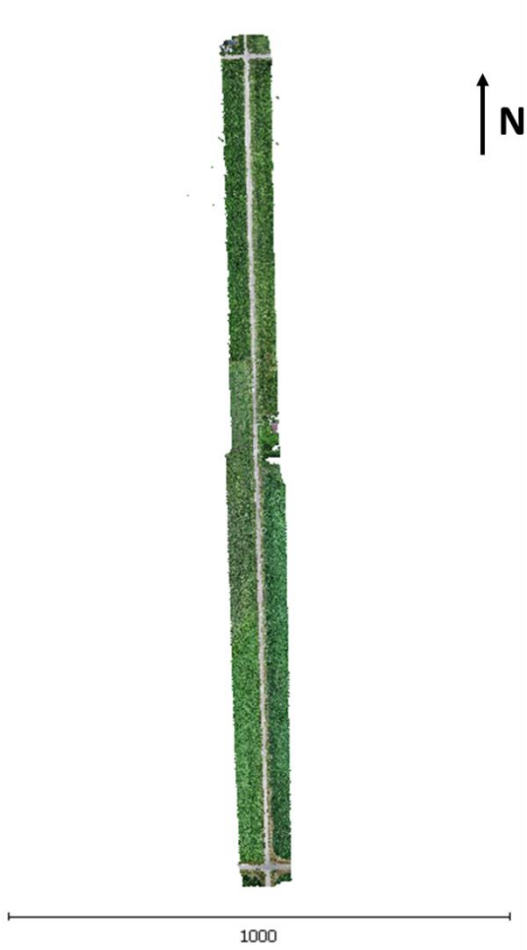

Figure 24. Processed UAS SfM collected on July 13, 2018 of N 162nd St. in Lancaster County (scale in meters).

Figure 25. Processed UAS SfM collected on Feburary 27, 2018 for 1900 St. in Saline County (scale in meters).

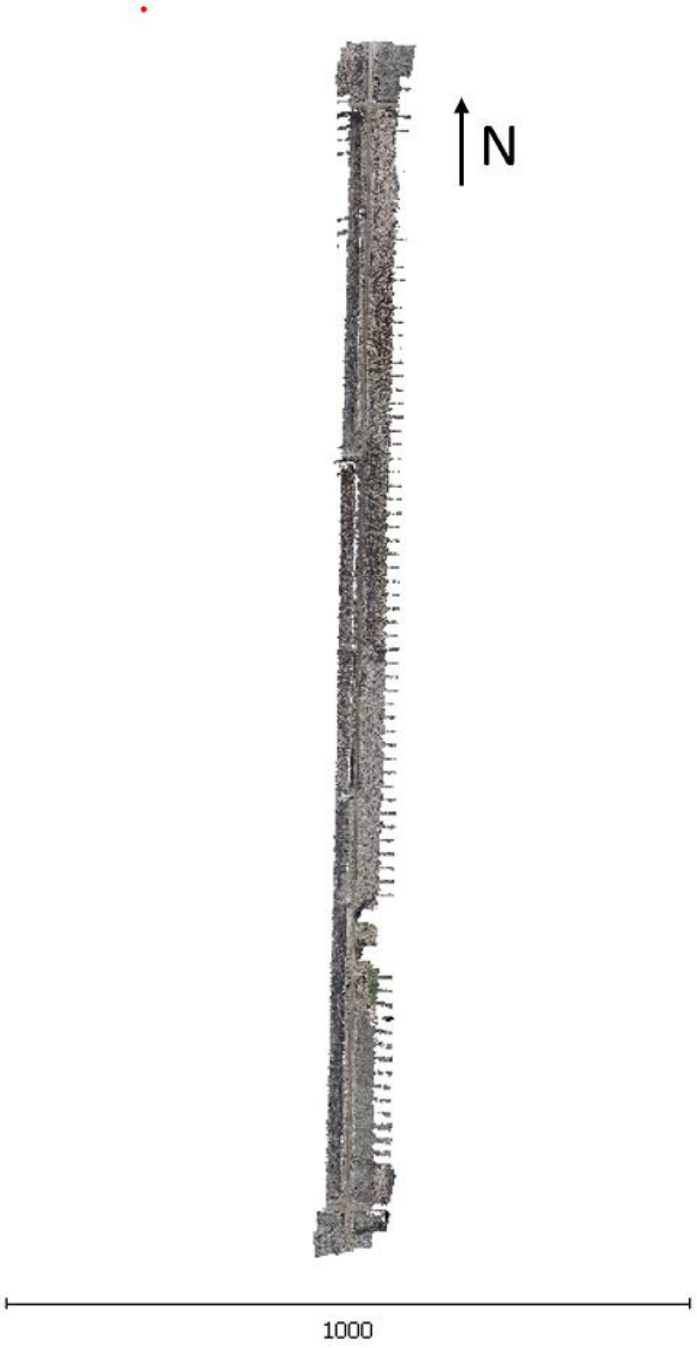

Figure 26. Processed UAS SfM collected on April 4, 2018 for 1900 St. in Saline County (scale in meters)

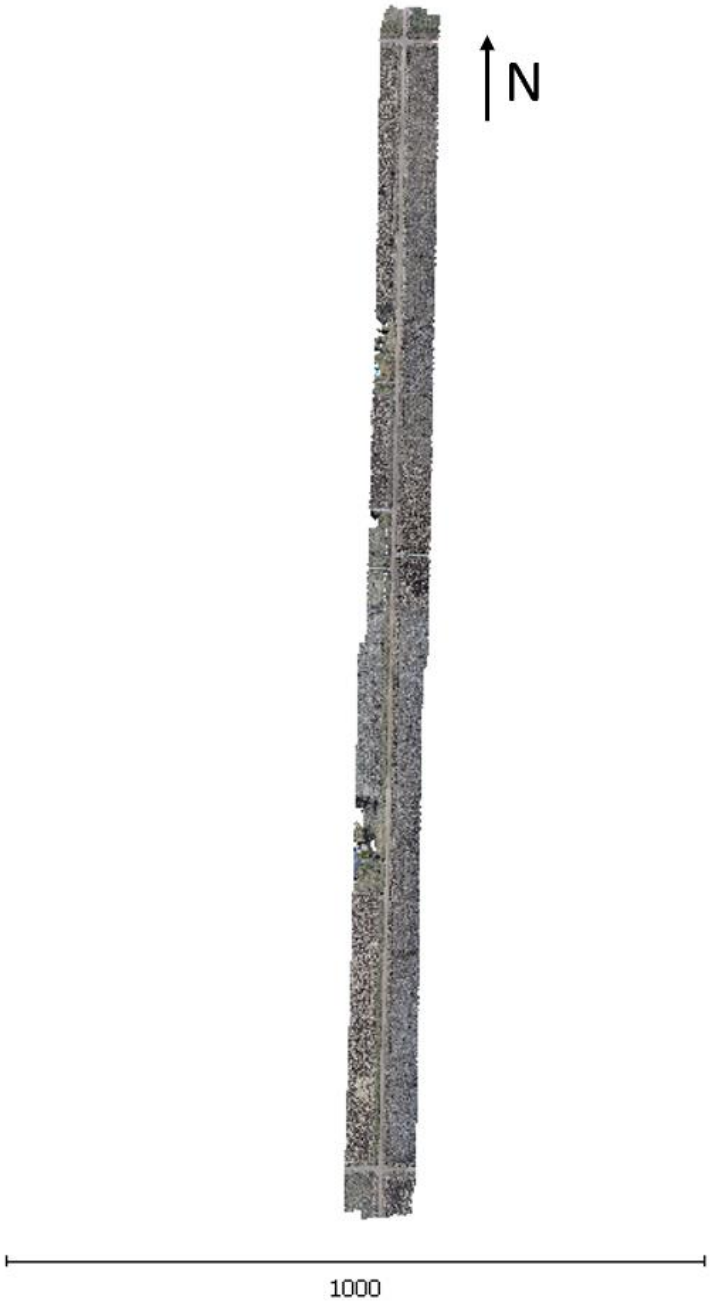

Figure 27. Processed UAS SfM collected on April 5, 2018, for 2300 St. in Saline County (scale in meters).

Table 15. Processed results of Waverly St. in Lancaster County on August 30, 2018.

Slope Values	**μ (%)**	**σ (%)**	**COV**
Positive	1.29	4.52	3.49
Negative	5.50	6.51	1.18

Table 16. Processed results of Waverly St. in Lancaster County on December 15, 2018.

Slope Values	**μ (%)**	**σ (%)**	**COV**
Positive	4.62	2.72	0.59
Negative	2.74	1.53	0.56

Table 17. Processed results of Waverly St. in Lancaster County on March 21, 2019.

Slope Values	**μ (%)**	**σ (%)**	**COV**
Positive	3.74	5.33	11.24
Negative	2.91	3.65	9.86

Table 18. Processed results of N 162nd St. in Lancaster County on April 22, 2019.

Slope Values	**μ (%)**	**σ (%)**	**COV**
Positive	4.45	1.21	0.27
Negative	0.6	1.57	2.61

Table 19. Processed results of N 162nd St. in Lancaster County on July 13, 2019.

Slope Values	μ (%)	σ (%)	COV
Positive	8.20E+04	1.50E+06	14.02
Negative	0.43	1.31	3.05

Table 20. Processed results of 1900 St. in Saline County on February 27, 2018.

Slope Values	μ (%)	σ (%)	COV
Positive	3.91	3.65	0.93
Negative	3.17	7.19	4.26

Table 21. Processed results of 1900 St. in Saline County on April 4, 2018.

Slope Values	μ (%)	σ (%)	COV
Positive	4.63	2.33	0.50
Negative	2.65	2.67	1.61

Table 22. Processed results of 2300 St. in Saline County on April 5, 2018.

Slope Values	μ (%)	σ (%)	COV
Positive	3.82	1.04	0.27
Negative	2.87	1.19	0.64